







## RESEARCH ARTICLE OPEN ACCESS

# Industrial Scale Production and Characterization of a Whey Fraction Enriched in Extracellular Vesicle Material

Søren Roi Midtgaard<sup>1</sup>  | Maria Stenum Hansen<sup>1</sup>  | Nikolaj Drachmann<sup>1</sup> | Xiaolu Geng<sup>1</sup>  |  
 Kristine Ingrid Marie Blans<sup>1</sup>  | Manja Mahmens Fabricius Møbjerg<sup>1</sup> | Anny F. Frølund<sup>1</sup> | Jan Trige Rasmussen<sup>2</sup>  |  
 Marie Stampe Ostenfeld<sup>1</sup> 

<sup>1</sup>Arla Foods Ingredients Group PS, Viby, Central Jutland Region, Denmark | <sup>2</sup>Aarhus Universitet, Aarhus, Central Jutland Region, Denmark

**Correspondence:** Søren Roi Midtgaard ([soemi@arlafoods.com](mailto:soemi@arlafoods.com))

**Received:** 9 July 2024 | **Revised:** 25 February 2025 | **Accepted:** 1 March 2025

## ABSTRACT

Human milk serves the sole nutritional role for the developing infant. During lactation, nano-sized extracellular vesicles (EVs) in milk containing a multitude of biologically active components are transferred from mother to offspring. Infant formula (IF) based on cow milk-derived ingredients has been reported to contain reduced levels of EVs as compared to human milk. There is therefore an unmet need to produce large-scale volumes of milk EVs to improve IF composition.

Here, we report a scalable industrial production protocol for a bovine whey-derived ingredient that is highly enriched in EV material using a large-scale sequential ceramic membrane filtration setup. Furthermore, we demonstrate a robust and generally applicable analytical approach to determine the relative contributions of EVs and milk fat globule membrane (MFGM) using molar ratios of the membrane-bound proteins butyrophilin (BTN) and CD9 as surrogate markers for MFGM and EVs, respectively. Taken together, our findings provide a basis for comparing bovine milk-containing foods and aid in developing specialized ingredients that can minimize the compositional difference between infant formula and human milk.

## 1 | Introduction

Exclusive breast feeding for the first 6 months of life is recommended by the World Health Organization (World Health Assembly 55 2002), highlighting that milk is comprised of everything necessary for optimal infant growth and development (Ballard and Morrow 2013; Harzer et al. 1983; Claumarchirant et al. 2016). Even though substantial efforts have been made to mimic breast milk composition (Martin et al. 2016), formula-fed infants still show considerable differences in gut microbiota composition, growth patterns, and prevalence of infections compared to breastfed infants (Quigley et al. 2016; Forbes et al. 2018; Lönnerdal 2010). Advantages in cognitive function have also been observed in breastfed infants compared to formula fed infants (Anderson et al. 1999), suggesting that infant formulas can be improved for optimal neuronal and cognitive development (Timby et al. 2014). Polar lipids, especially sphingomyelin (SM), have often been

associated with optimal infant neurodevelopment (Schneider et al. 2019), and supplementing infant formula with polar lipids from the membrane enveloping milk fat globules (milk fat globule membrane—MFGM) shows well documented health benefits in infants, including improved neuro- and cognitive development (Timby et al. 2014, 2021; Li, Hock, et al. 2019; Li, Wu, et al. 2019), fewer incidences of diarrhoea (Zavaleta et al. 2011), protective immunological and metabolic effects (Lee et al. 2018; Timby et al. 2015), and a microbiome closer to resembling breastfed infants (Demmelmair et al. 2017; Bhinder et al. 2017). Taken together, there is still a need to develop formulas and their lipid containing ingredients further in an effort to eliminate these differences. Here we focus on a subcomponent of milk, namely the extracellular vesicles (EVs) (Admyre et al. 2007).

The phospholipids in bovine milk are generally described to be constituted of 60% MFGM, while the remaining 40% belongs to

This is an open access article under the terms of the [Creative Commons Attribution-NonCommercial-NoDerivs](https://creativecommons.org/licenses/by-nc-nd/4.0/) License, which permits use and distribution in any medium, provided the original work is properly cited, the use is non-commercial and no modifications or adaptations are made.

© 2025 Arla Foods Ingredients Group P/S and The Author(s). *Journal of Extracellular Biology* published by Wiley Periodicals LLC on behalf of International Society for Extracellular Vesicles.

the skim milk phase (Patton and Keenan 1971)—suggesting up to 40% EV material. The phospholipids in the skim milk phase are likely a mixture of small MFGs, MFG-detached MFGM, and EVs, including sub-EV populations of both small EVs (30–150 nm) and large EVs (100–1000 nm) (Admyre et al. 2007). These vesicle-type particles are secreted into the milk by mechanisms distinct from MFG biogenesis and secretion (see Figure 1 for a biogenesis overview) with a small contribution likely originating from the lymphocytes and macrophages found in milk (Van Herwijnen et al. 2016; Buratta et al. 2023). While the core of the milk fat globules (MFGs) is primarily comprised of triacylglycerols (TAG), the lumen of EVs contains ribonucleic acid (RNA) and cytosolic proteins. The MFGs are coated with a triple-layer of phospholipids, with the inner monolayer originating from the endoplasmic reticulum and the outer bilayer originating from the plasma membrane (Cavaletto et al. 2008). The phospholipid bilayer surrounding exosomes originates from the endosomal system, whereas microvesicles are enveloped by the plasma membrane during secretion. EVs are actively secreted into the milk, where they are involved in cell communication by transporting signalling molecules between cells, tissues, and between mother and child (Hata et al. 2010; Sanwlani et al. 2020; Chen et al. 2016). In general, the EV content reflects the parent cell, but cargo sorting and packaging of specific components into EVs appear to be a regulated process with various mechanisms involved (reviewed here: Chen et al. 2021; Anand et al. 2019). Thus, bovine EVs comprise a potential source of essential bioactive phospholipids, which in infant formula can supplement MFGM to more closely match the dynamic composition of milk lipids during a feeding (van Sadelhoff et al. 2018; Takumi et al. 2022) and over the lactation (Harzer et al. 1983; Claumarchirant et al. 2016). The aspect of adjusting the MFGM and EV ratio is largely overlooked in modern formula manufacturing due to the lack of available ingredients and analytical knowledge (Santoro et al. 2023).

EVs have been isolated from a variety of milk sources, including human, bovine, pig and sheep milk (Admyre et al. 2007; Reinhardt et al. 2012; Gu et al. 2012; Wooding 1974; Mecucci et al. 2020, 2021), and the most abundant miRNAs in milk EVs appear to be conserved between species with implications on immunological cell responses (van Herwijnen et al. 2018; Izumi et al. 2015; Sun et al. 2013). Due to the complex milk matrix, with components overlapping EV size and density, isolation methods often include several number of steps starting with an initial crude separation of colloidal structures such as MFGs, cell debris and casein micelles, for example, by centrifugation (Blans et al. 2017) or acidification (Rahman et al. 2019; Morozumi et al. 2021). Further separation of EVs can be obtained by applying precipitation, ultracentrifugation, or density gradients (Wadenpohl et al. 2024; Lane et al. 2017; Yuan et al. 2023). These purification protocols have been optimized to include methods easily applied in small-scale isolations. However, with an increasing interest in milk-derived EVs for infant nutrition and natural delivery vehicles for therapeutic drugs, there is a need to investigate the potential of industrial scale dairy streams as a source of EVs (Paolini et al. 2022). Membrane filtrations are efficiently utilized at an industrial scale to separate molecules according to sizes, and sequential filtration has been used on a small scale to gently obtain an enriched EV fraction (Heinemann and Vykoukal 2017). It is well-known that the choice of isolation

method and pre-processing of raw material is crucial to preserve EV integrity (Théry et al. 2018). This is of particular importance for the infant formula manufacturers, where research shows that EVs exist in infant formulas but are compromised compared to native skim milk EVs (Mukhopadhyaya et al. 2021). Thus, as also highlighted by the International Society of Extracellular Vesicles (Paolini et al. 2022), there is a need for an optimized, large-scale isolation method to obtain an EV-enriched fraction from bovine milk.

In the present study, an industrially relevant method to enrich EVs from acid whey by serial filtration is presented. The enriched isolate is assessed for the relative content of EV and MFGM material by introducing a ratio of the two membrane protein markers, CD9 and butyrophilin (BTN), respectively. By three complementary analytical approaches, the ratio of BTN/CD9 is successfully used to describe the relative distribution of MFGM and EV material in different industrial milk fractions, including the presented EV-enriched fraction from acid whey. To the best of our knowledge, this study is the first to introduce an industrial large-scale isolation and characterization of milk-derived EVs for utilization in infant nutrition.

## 2 | Materials and Methods

### 2.1 | Parallel Filtration

Bovine skim milk was first concentrated to 4.5% protein and 0.08%–0.11% fat by a combination of filtration and evaporation. Acid whey was produced by mineral acidification of the skim milk using HCl, according to published protocols (Bylund n.d.). The majority of the minerals, non-protein-nitrogen (NPN) and lactose were removed from the thin whey by filtration to 82% protein of total solids.

Before further processing, the acid whey was diluted from 27% total solids (TS) to a concentration of 9% TS before pH adjustment to pH 6.5 using a mix of 2/3 NaOH and 1/3 KOH. A parallel filtration was performed using a trisampler, which enables running three membranes in parallel. Two runs were performed. One with TAMI ISOFLUX 23 channel membranes (1.4, 1.2 and 0.8 µm, respectively), and one with TAMI ISOFLUX 23 channel membranes (0.45, 0.20, and 0.14 µm, respectively). In each case, the membranes were mounted in the trisampler.

The two filtrations were performed at a feed pressure of 2 bar and a permeate pressure of 2.4 bar. Both the retentates and the permeates were directed back to the feed tank to ensure a stable feed during the experiments, and the system was left to equilibrate for 3 h before samples were collected for analysis. After equilibration, permeate samples were taken for analysis. An overview of the setup and composition of feed and permeate samples of the different membranes can be found in Figure S1 and Table S1.

### 2.2 | Serial Filtration

Bovine acid whey was used as starting material for the serial filtration setup. The acid whey was produced according to the

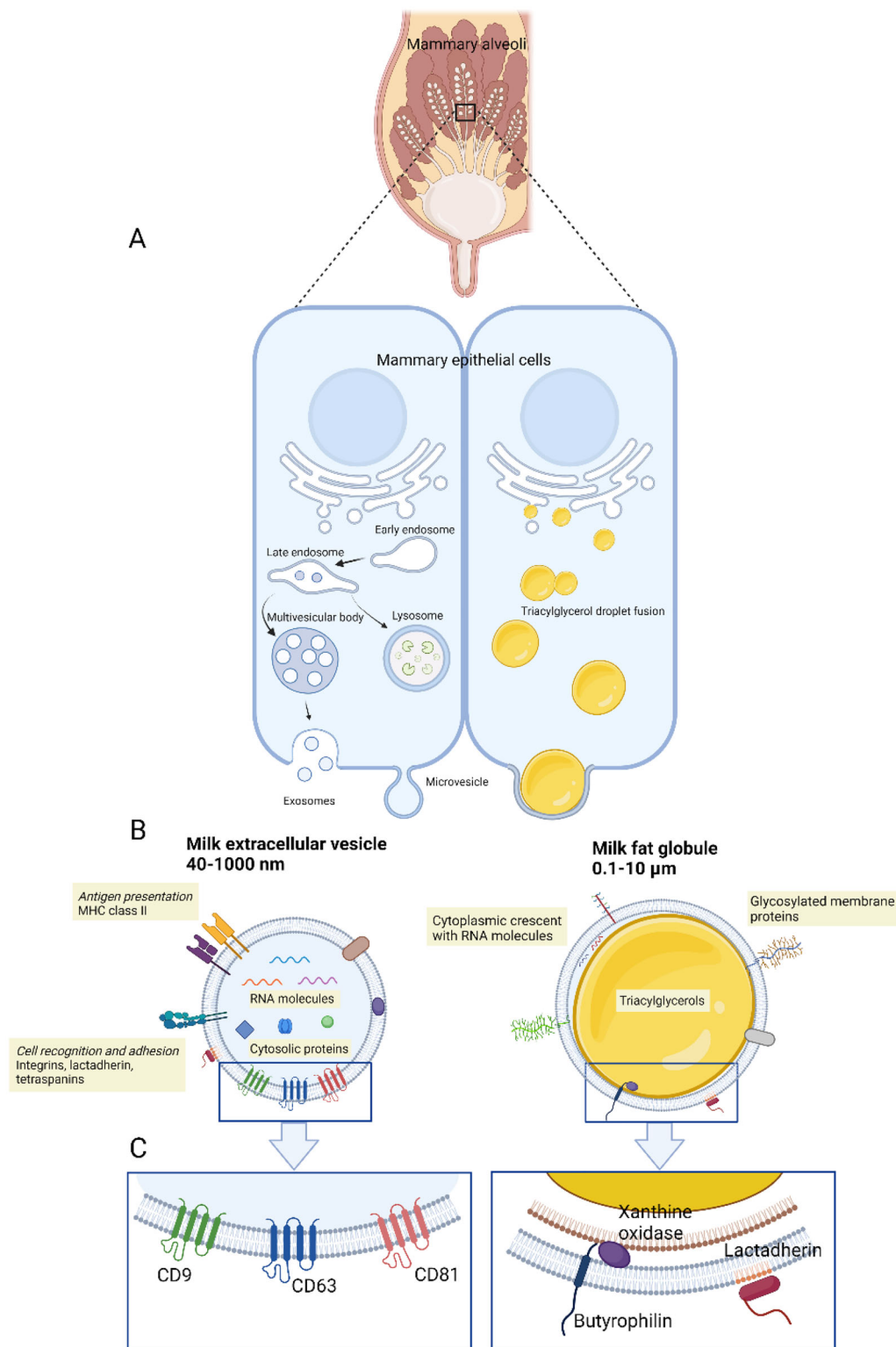


**FIGURE 1** | Milk EV and MFG biogenesis from mammary epithelial cells and composition. (A) Exosomes are formed by invaginations of the endosomal membrane creating intraluminal vesicles kept in multivesicular bodies, which upon fusion with the plasma membrane release the vesicles to the milk matrix as exosomes. Microvesicles are released into milk by direct outward membrane budding from the plasma membrane. TAGs are synthesized and released from the endoplasmic reticulum as small droplets enveloped by a single phospholipid layer. These fuse and grow in size during transportation towards the apical plasma membrane. Here, the lipid droplets are further enveloped by the apical cell membrane, resulting in a tripartite membrane coating the MFGs called MFGM. MFGs comprise more than 98% of the lipid mass in milk and serve an important purpose as a TAG-containing energy-dense fraction. (B) Composition of a generic EV with a phospholipid bilayer embedded with membrane-associated proteins and intraluminal content of RNA molecules and cytosolic proteins. The MFG has a core of TAG surrounded by the MFGM containing membrane-associated proteins with a possible content of cytoplasmic crescent containing RNA and cytosolic proteins. (C) Inserts depict the main different membrane protein markers in focus of this study. EV, extracellular vesicles; MFG, milk fat globule; MFGM, milk fat globule membrane; RNA, ribonucleic acid; TAG, triacylglycerols.

same procedure as described for the parallel filtration. The composition of the acid whey starting material is found in Table S2.

Before further processing, the acid whey was diluted from 27% total solids (TS) to a concentration of 9% TS before pH adjustment to pH 6.5 using a mix of 2/3 NaOH and 1/3 KOH. Filtration was performed using TAMI 0.45 µm ISOFLUX 23 channel membrane at a feed pressure of 2 bar and permeate pressure of 2.25 bar. Four hundred percent diafiltration (calculated based on starting feed volume) was performed using polished water (water filtered by reverse osmosis to obtain a conductivity of at most 0.05 mS/cm) as the diafiltration medium. The temperature of the feed, the permeate, and the retentate during the microfiltration was approximately 10°C. After the diafiltration was performed, a final concentration step of the retentate was performed to increase the TS concentration in the retentate. The composition of the corresponding retentate and permeate from the filtration is found in Table S2.

The permeate from the first filtration was collected and used as feed for a second filtration performed using TAMI 0.20 µm ISOFLUX 23 channel membrane. The second filtration was performed with the same running settings as the first filtration, except only 300% diafiltration was performed. Also here, a final concentration step was included after the diafiltration to increase the TS concentration in the retentate. The composition of the corresponding retentate and permeate from the 0.20 µm microfiltration is found in Table S2.

The permeate from the second microfiltration was collected and used as feed for a final ultrafiltration step, in order to concentrate the soluble protein fraction. This was performed using Koch HFK328 31D 5 KD membrane at a feed pressure of 3 bar and a pressure drop of 1 bar per element. The composition of the retentate from the filtration step can be found in Table S2.

Finally, the 0.45 µm retentate and 0.20 µm retentate were dried by freeze drying, and the retentate from the ultrafiltration was dried by spray drying. All powders were stored at −80°C until further use. The process for obtaining the 0.20 µm retentate (the so-called novel cholesterol-enriched milk lipid composition suitable for infant nutrition) has been used for applying for a processing patent (WO 2022/112552). In the present text, this fraction is referred to as the acid whey EV fraction (AW-EV).

## 2.3 | Western Blotting

Equipment/reagents and chemicals were bought from BioRad unless otherwise stated. Powdered samples (see sample overview in Figure S2) were dissolved in Milli-Q water, and both liquid and powdered starting material were appropriately diluted before mixing with Laemmli sample buffer. For reduction, 80 mM dithiothreitol (DTT) was added. All samples were subsequently heated for 5 min at 100°C and stored at −20°C until further use. Protein separation was conducted by SDS-PAGE using 8%–16% Mini-PROTEAN TGX gradient gels and Tris/Glycine/SDS running buffer. After separation, proteins were transferred to 0.2 µm-polyvinylidene difluoride membranes (100 V for 1 h) and subsequently blocked in 3% gelatin dissolved in TBS containing

0.5% Tween 20. Probing with primary antibody was conducted overnight at 4°C. Secondary alkaline phosphatase-antibodies were used to detect target proteins by a colorimetric reaction with 5-bromo-4-chlor-indolylphosphate and nitro blue tetrazolium.

The following antibodies were used: monoclonal mouse anti-human CD9 (clone IVA50, reducing conditions; diluted 1:1000; ThermoFischer), monoclonal mouse anti-bovine CD63 (clone CC25; non-reducing conditions; diluted 1:2000; ThermoFischer), monoclonal mouse anti-human CD81 (clone 12C4; non-reducing conditions; diluted 1:1000; CosmoBio), monoclonal rabbit anti-bovine BTN (clone 102.43; reducing conditions; diluted 1:1000; LSBio), polyclonal rabbit anti-human XOD (reducing conditions; diluted 1:1000; Abcam), and polyclonal rabbit anti-bovine lactadherin (reducing conditions; diluted to 1 µg/mL; in house-produced by Jan Trige Rasmussen, Aarhus University).

For comparative quantitative evaluation, the appropriate amount of protein loaded onto the gels was individually assessed for all samples. Six identical SDS-PAGE gels were run with all samples. Subsequently, three gels were blotted with the CD9 antibody and three gels with the BTN antibody. The blots were scanned into high-quality TIF images, and band intensities were quantified using Fiji (ImageJ) (Schindelin et al. 2012) software using the gel analyser feature. Results are seen in Figure 4A, Figure S4 and Figure 5A.

## 2.4 | Mass Spectrometry (MS)

The target peptides were selected based on the uniqueness of the tryptic peptide sequence (obtained by in silico trypsin digestion using the peptide-mass tool and protein sequences obtained from [https://web.expasy.org/peptide\\_cutter/](https://web.expasy.org/peptide_cutter/)), the ability to detect these peptides using MS, and the absence of readily oxidizable cysteine and methionine residues and post-translational modification sites such as serine and threonine amino acid residues. The peptide sequences were also limited to no more than 15 amino acid residues. The selected peptides are shown in Table 1 below.

The selected peptides (both light/native and heavy/labelled) were purchased from Thermo Fisher Scientific as HeavyPeptide AQUA Ultimate grade. For internal standards, the last AA of the peptide was labelled with <sup>13</sup>C and <sup>15</sup>N, thereby producing a mass shift between the heavy labelled and the native peptide of +10 for arginine and +8 for lysine.

Samples were solubilized in 50 mM triethylammonium bicarbonate (TEAB) (Merck) pH 8.5 to give a concentration of 1.5 mg/mL protein. A 100 µL sample was reduced with dithiothreitol (DTT) (Merck) (40 µL of 100 mM) for 30 min at 100°C and alkylated with iodoacetamide (IAA) (140 µL of 100 mM) (Merck) for 30 min at RT in the dark. Proteins were digested by incubation with trypsin (T1426, Merck) (1:20 w/w) for 4 h at 37°C. The samples were acidified with trifluoroacetic acid (TFA) (Merck) (final concentration 0.3% v/v) to stop the hydrolysis. Labelled synthetic peptides (BTN\_411-420\* and CD9\_169-175\*) were spiked into the standard solutions and the acid hydrolysed samples at a concentration of 100 and 30 nM, respectively. Prior to injection, the samples were filtered through a 0.22 µm syringe filter, and an internal standard was added.



**TABLE 1** | Overview of the peptides used for quantification by mass spectrometry.

Protein	Protein ID	Peptide position	Peptide sequence	Fragmentor [V]	Precursor ion à Product ion	CE [mV]
Butyrophilin (BTN)	P18892	411–420	TPPLAGPPR	141	509.8 à 707.4	18
		411–420*	TPPLAGPPR	141	514.8 à 717.4	18
CD9	P30932	169–175	NLIDSLK	141	401.7 à 575.3	5
antigen (CD9) CD63		169–175*	NLIDSLK	141	405.7 à 583.3	5
CD81	Q9XSK2	157–163	ILAVTNK	141	379.7 à 645.4	7
Lactadherin (LAH)	Q3ZCD0	23–36	LAGGVILGVALWLR	141	719.5 à 1040.66	22
Xanthine oxidase (XOD)	Q95114	339–348	VTGITQGAR	141	508.3 à 645.4	13
	P80457	311–318	TLLEAVAK	141	422.8 à 630.4	6

\*indicates the heavy/labelled peptide.

Peptides were separated on an Agilent 1200 Series HPLC system equipped with a RP Symmetry300 C18 column (5 µm, 2.1 mm × 150 mm) and a guard column (VanGuard Cartridge, Symmetry 300 C18, 5 µm, 2.1 mm × 5 mm); both columns from Waters, with a flow rate of 0.35 mL/min for 60 min. The aqueous mobile phase (A) contained 0.1% formic acid (FA) (VWR International), and the organic mobile phase (B) contained 0.1% FA in acetonitrile (ACN) (Rathburn). Standards and samples (20 µL) were loaded onto the column with 3% mobile phase B for the first 2 min. Peptides were eluted from the column with a gradient of 3%–29.4% B over 23 min, increasing to 100% B over 10 min. After 10 min at 100% B, the column was re-equilibrated at the initial conditions for a period of 15 min. The column temperature was maintained at 45°C.

The Agilent 1200 Series HPLC system was coupled directly to an Agilent 6410 Triple-Quad mass spectrometer (Agilent Technologies) using a positive electrospray ionization (ESI) interface. ESI conditions were as follows: Gas temperature 300°C, gas flow 10 L/min, nebulizer gas pressure 35 psi, capillary voltage 4000 V, delta EMV (+) 600 V, cell accelerator voltage 7 V. The 6410 triple Q was operated in MRM mode with selected fragmentor voltage and collision energy as described in Table 1. Transition masses of the precursor ions detected in the first quadrupole (Q1) and the fragment ions detected in the second quadrupole (Q3) for each peptide (BTN\_411-420 and CD9\_169-175) were submitted as a batch for data acquisition. Quantification was calculated based on the ratio of the analyte and internal standard by MassHunter Quantitative Analysis software (Agilent Technologies) and Excel (Microsoft) using serial standard concentrations for BTN\_411-420 and CD9\_169-175, which were 10, 50, 100, 150 and 200 nM and 1, 10, 30, 40 and 50 nM, respectively. Plots demonstrating the linearity of the quantification are found in Figure S6.

## 2.5 | Transmission Electron Microscopy (TEM)

The lab-scale pure MFGM and EVs samples were first thawed on wet ice and diluted 1:1 with 1× PBS (pH 7.2) before being fixed in 2% glutaraldehyde phosphate buffer (pH 7.2) for 60 min at room temperature, and centrifuged at 100,000 × g for 90 min at 15°C. The pellet was gently taken out and submerged in warm (38°C) 2% low melting agarose (Carl Roth, Germany) and left at room temperature for solidification. The pre-treatment of the sample was done in duplicate.

For the 3 fractions obtained from pilot production, the samples were first centrifuged at 3400 × g at 4°C for 35 min to remove protein aggregates. The supernatant was further centrifuged at 170,000 × g for 90 min at 15°C, and the pellet was resuspended in 1× PBS (pH 7.2) and fixed with 2% glutaraldehyde phosphate buffer (pH 7.2) for 60 min at room temperature. Thereafter, the sample was centrifuged again at 170,000 × g for 90 min at 15°C, and the pellet was put in 2% low melting agarose and left at room temperature for solidification. The pre-treatment of the sample was done in duplicate.

Further TEM sample preparation was done following the same process used by Bach Korsholm Knudsen et al. (2021). Briefly, the sample in agarose was cut in to small pieces, washed and postfixed in 1% w/v OsO<sub>4</sub> with 0.05 M K<sub>3</sub>Fe(CN)<sub>6</sub> in 0.12 M phosphate

buffer (pH 7.2) for 2 h. This was followed by a standard procedure for dehydration, embedding, and sectioning. The copper grids with Formvar supporting membranes were used for collecting the sectioned samples. Subsequently, stained with uranyl acetate and lead citrate, and examined by a Philips CM-100 electron microscope (Philips, Eindhoven, The Netherlands) operated at 100 kV.

## 2.6 | Immunogold Electron Microscopy (iEM)

Milk-derived samples were mixed 50:50 with 4% paraformaldehyde for 10 min, and subsequently 10  $\mu$ L of the fixed sample was deposited on a formvar supported one-whole copper grid and allowed to adsorb for 5 min. Following blotting of the sample with filter paper, the grid was deposited on a 25  $\mu$ L drop of pre-incubation medium (PBS + 1% BSA + 0.05 M glycine) on parafilm for 10 min. Following a wash (PBS + 1% BSA), the grid was deposited on a 25  $\mu$ L drop of primary antibody in PBS + 1% BSA in a humidity chamber for 24 h at 4°C. Following a wash (PBS + 1% BSA), the grid was deposited on a 25  $\mu$ L drop of secondary antibody made from a 25 mL solution of TBS (0.05 M Tris + 0.1% BSA) + 10 nm gold labelled Protein A (1.5 mL of 1% PEG) + 1% cold water fish gelatin on Parafilm. The grids were washed in TBS and subsequently distilled water, stained with 2% uranyl acetate for 15 min, and subsequently examined with a Philips CM 100 Transmission EM (Philips, Eindhoven, The Netherlands), operated at an accelerating voltage of 80 kV. Digital images were recorded with an OSIS Veleta digital slow scan 2k  $\times$  2k CCD camera and the ITEM software package. Images were analysed using Fiji (Schindelin et al. 2012), employing the 'analyse particles' feature on binary watersheded pictures with a predetermined size (in pixel units). Out of a pool of 50 pictures for each sample and antibody, at least 10 pictures with a scalebar of either 1 or 0.5  $\mu$ m were counted for positive gold labels (black spots of the expected size) and averaged by area to produce a value of [gold particles per area]. Representative pictures are shown in Figure 4B.

## 2.7 | General Compositional Analysis

### 2.7.1 | Total Solids

The total solids were determined according to NMKL 110 2nd edition, 2005 (Total solids (Water)—gravimetric determination in milk and milk products). NMKL is an abbreviation for 'Nordisk Metodikkomite for Næringsmidler.'

### 2.7.2 | Total Protein

(1) Determining the total nitrogen of the sample following ISO 8968-1/2 (IDF 020-1/2-Milk Determination of nitrogen content—Part 1/2: Determination of nitrogen content using the Kjeldahl method). (2) Determining the non-protein nitrogen of the sample following ISO 8968-41 / IDF 020-4.

Determination of nitrogen content—Part 4: Determination of NPN content. The total protein is then calculated by subtracting the two values and using a Kjeldahl factor of 6.38.

### 2.7.3 | Ash

The ash content of a food product is determined according to NMKL 173: 2005 'Ash, gravimetric determination in foods.'

### 2.7.4 | Total Phospholipid

Quantitative analysis was performed using  $^{31}\text{P}$  NMR by Spectral Service AG.

### 2.7.5 | Total Triacylglycerol (TAG)

Standard Rose Gottlieb analysis minus the total phospholipid.

## 3 | Results

### 3.1 | Industrial-Scale Isolation of a Milk-Enriched Fraction in EV Material

Two types of whey were initially explored as potential raw material for isolation of milk EV material (see milk processing diagram in Figure S2 for an overview and more information). Sweet whey (a byproduct from cheese production obtained by casein micelle removal through enzymatic-mediated precipitation) and acid whey (a byproduct from caseinate production obtained by HCl-mediated precipitation of the casein micelles in concentrated skim milk) were examined by electron microscopy (data seen in Figure S3). Visual inspection revealed the presence of EV-type structures, identified by their electron-dense (black) lipid-bilayer-like perimeter and a central lighter core. These EV-like structures were observed in both types of whey. Furthermore, small particles with a uniform electron density indicated the presence of small MFGs of similar size to EV, especially in the sweet whey. Suspecting that the similar size would complicate the production of an EV-enriched fraction, acid whey was chosen as a starting material for further processing. Next, ceramic filter membranes of increasing cut-off pore sizes (0.14, 0.20, 0.45, 0.8, 1.2 and 1.4  $\mu$ m) were tested in a parallel filtration setup using acid whey as input to identify the optimal membrane cut-off for isolation of EVs (overview and data in Figure S1 and Table S1, respectively). Here it should be noted that there is a significant difference in permeation between polymeric and ceramic membranes, as demonstrated by Zulewska et al. (2009). Based on macro-component analysis, ceramic membranes of 0.45  $\mu$ m, 0.2  $\mu$ m, and a 5 kDa pore-size were chosen for further optimization of isolation.

In order to avoid changes in surface charge interactions during processing, acid whey was first adjusted to pH 6.5, whereafter a serial filtration scheme was established on an industrial pilot plant scale. As outlined in Figure 2A, progressively smaller pored membranes were used, and diafiltration was conducted for continuous particle enrichments. For example, the *retentate* from 0.45  $\mu$ m filtration was collected, and the 0.45  $\mu$ m *permeate* was subsequently used as input feed for 0.20  $\mu$ m filtration and so forth. The retentates obtained were named 'MFG fraction,' 'EV fraction,' 'Soluble protein fraction' and 'permeate fraction,' based on their putative relative enrichment of MFG, EVs, soluble proteins,

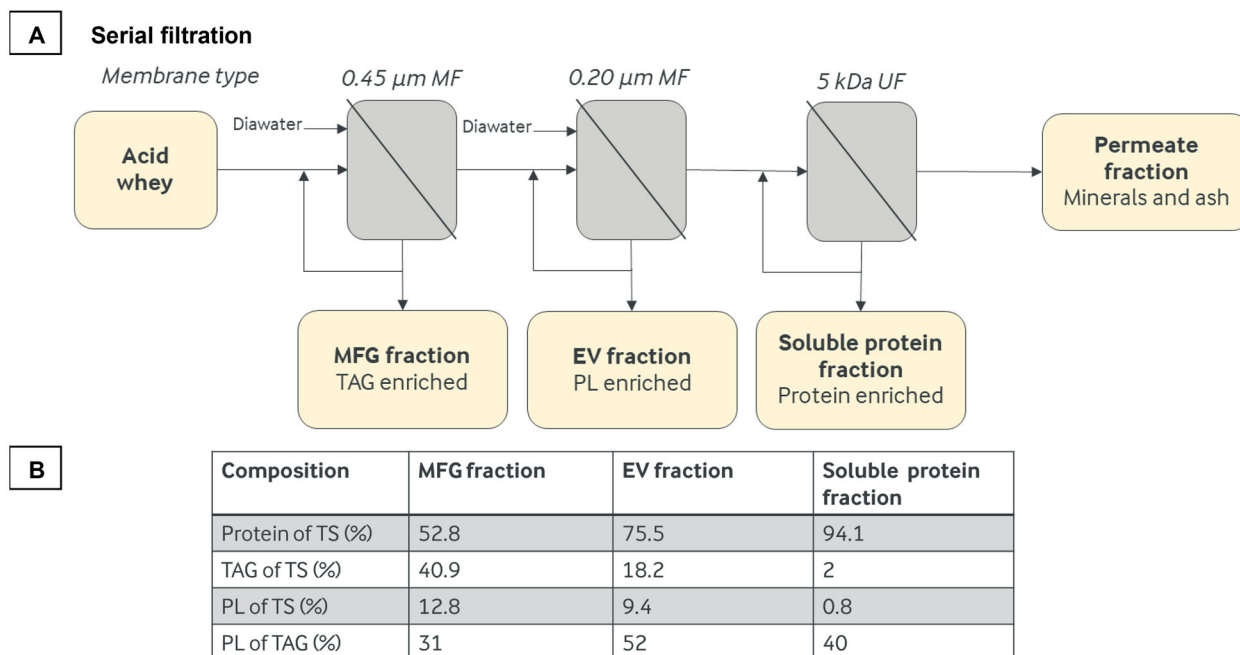


**FIGURE 2** | Industrial scale isolation and characterization of (lipid)-enriched fractions/obtained from acid whey after serial filtration steps). (A) Depicts the series of filtrations using acid whey as feed/starting material and the fractions obtained after using different membrane pore sizes. MFG, EV, TAG, and phospholipids (PL). (B) The fractions were characterized for their protein composition and total solids (TS).

and permeate, respectively. Figure 2B describes overall macro-component content in the obtained fractions (Table S2, additional compositional information), except the permeate fraction that was disregarded. The MFG and EV fractions contained  $\geq 10\%$  of phospholipids per total solids, while the soluble protein fraction contained  $< 1\%$  phospholipids per total solids. Furthermore, the MFG fraction contained twice the amount of triglycerides than the EV fraction (40% vs. 18%), and a factor of 20 $\times$  more than the soluble protein fraction (40% vs. 2%). Finally, the total protein content per total solids gradually increased from  $\sim 50\%$  (MFG) to  $\sim 75\%$  (EV) and 94% (soluble protein fraction).

These data suggest that the majority of the MFGs were in the MFG fraction and that the protein content was inversely proportional to the phospholipid and TAG content—indicating that the majority of the proteins were in the soluble protein fraction. Moreover, the majority of phospholipid material per total lipids was detected in the EV fraction. Although exclusive separation of different constituents was not possible, relative enrichments in the fractions were obtained, and 0.5 kg freeze-dried powder of the EV fraction was obtained for further analysis.

### 3.2 | TEM Analyses of MFGM and EV Material

In order to gain further compositional insight into the three retentate fractions, we employed TEM to assess the nano-structures present. For reference purposes, we also purified pure MFGM material from cream and pure EV fractions from skim milk, both made using a lab-scale procedure as previously described (Blans et al. 2017). Representative pictures are shown in Figure 3 for all five samples. Visual inspection of the reference samples reveals that the Pure EV sample contains higher amounts of smaller EV-like structures, while the pure MFGM sample contains

many elongated structures and only very few smaller circular structures. In the three industrial-scale produced fractions, the elongated structures are mainly found in the MFG fraction, while the EV fraction seems to consist of more semi-circular vesicle-like structures. The partially collapsed morphology of the EVs is likely due to the high-speed centrifugation steps used in the TEM protocol. Previous micrographs of the pure EV and pure MFGM samples show the expected circular/spherical morphology (Blans et al. 2017). Finally, the soluble protein fraction consists of comparatively smaller particles with more uniform density. Taken together, this seems to qualitatively indicate that the desired enrichments have been obtained.

### 3.3 | Establishment of a Quantitative LC-MS Method of Membrane Marker Proteins to Delineate Origin of Membrane Material (EV vs. MFGM)

To acquire more robust and quantitative knowledge regarding the origin of the phospholipid-containing membranes observed by TEM, we identified suitable membrane-associated marker proteins for quantification of EV versus MFGM content. This provided quantitative, in-depth knowledge while also producing a more reproducible and inter-study comparable dataset, as put forth by iSEV (Nieuwland et al. 2022). From the bovine milk literature (Blans et al. 2017; Reinhardt and Lippolis 2006; Reinhardt et al. 2013), we selected 3 putative markers for MFGM and 3 general tetraspanin markers for EVs; see Table 2. The selected EV markers are commonly used in the EV literature, recommended for EV characterization (Welsh et al. 2023), and among the top 100 identified EV proteins according to the Vesiclepedia website (Kalra et al. 2012). These six selected markers were initially assessed by Western blot analysis on the lab-scale purified EV and MFGM reference samples (see Figure 4A). Using an identical

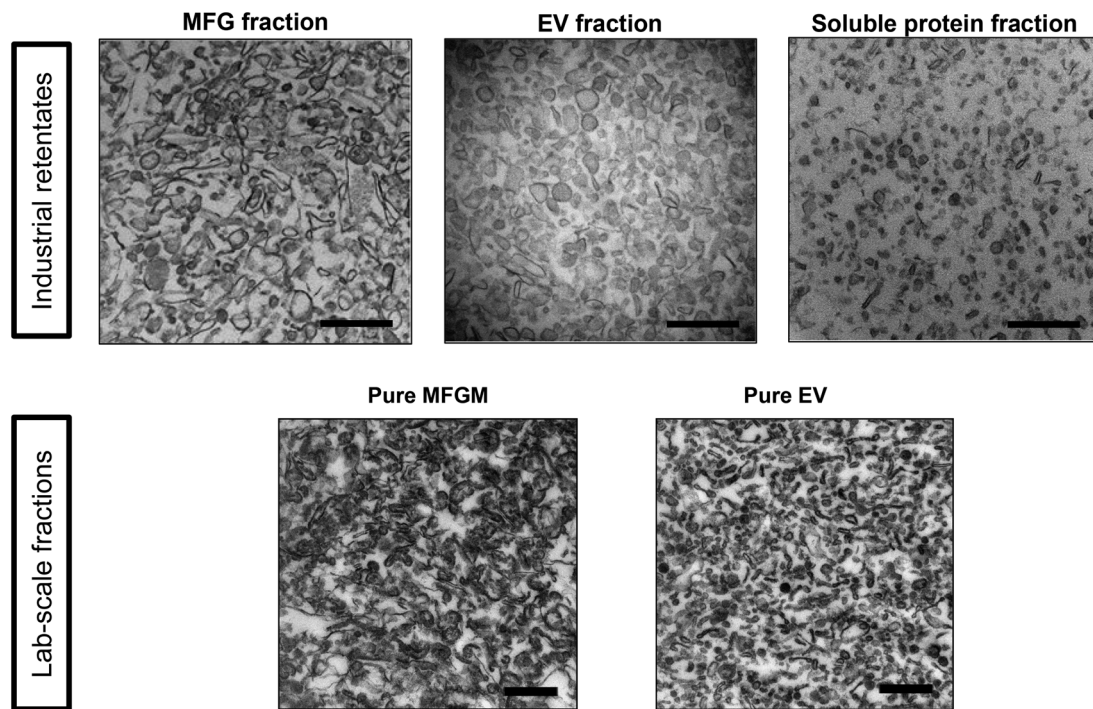


**FIGURE 3** | TEM micrographs. The upper row shows overview pictures of the three fractions obtained by sequential filtration. The lower row are pictures of the pure MFGM and EV reference samples. All scale bars are 500 nm. EV, extracellular vesicles; MFGM, milk fat globule membrane; TEM, transmission electron microscopy.

**TABLE 2** | MFGM and EV marker proteins used in this study.

	Protein name	UniProt reference	Mode of lipid interaction
MFGM markers	Butyrophilin 1 A1 (BTN)	P18892	Integral membrane protein
	Xanthine Oxidase/Dehydrogenase (XOD)	P80457	Membrane surface associated protein
	Lactadherin (LAH)	Q95114	Membrane surface associated protein
EV markers	CD9	P30932	Integral membrane protein
	CD63	Q9XSK2	Integral membrane protein
	CD81	Q3ZCD0	Integral membrane protein

Abbreviations: EV, extracellular vesicles; MFGM, milk fat globule membrane.

protein load, CD63 and CD81 proteins were seemingly unique markers for EVs, while CD9 was non-unique but still more prominently present in the EV sample compared to the MFGM sample. For the MFGM markers, none of the tested proteins were unique for the MFGM sample, but they all demonstrated significantly stronger signals for MFGM than for EV, confirming that the selected proteins are respective markers for MFGM and EV.

Next we established a quantitative MS method to quantify the membrane proteins using a protocol of tryptic peptides similar to previously published studies (Affolter et al. 2010; Bär et al. 2019; Fong and Norris 2009). For the three tetraspanins, we only obtained detection of CD9, and not from CD63 or CD81. Recent reports also seem to demonstrate that CD9 is the most abundant of the three tetraspanins (Mukhopadhyaya et al. 2021), consistent

with our findings. Based on our MS and WB data, we proceeded with CD9 as our general EV marker.

The three MFGM marker proteins were all detected and quantified based on tryptic peptides, as has also been described previously (Affolter et al. 2010; Fong and Norris 2009). If all three proteins were equally good MFGM markers, that would imply that they follow each other in a highly consistent molar ratio, independent of the sample investigated. To test this, we analysed the ratio between these three MFGM proteins in a diverse set of bovine milk-derived samples that were subjected to various levels of processing, including the Pure EV and MFGM lab-scale samples, and the industrial AW-EV fraction was also probed by TEM (see Figure S2 for a detailed production scheme and sample information and Figure S5 for the obtained molar ratios for all samples). For BTN and XOD, we found an approximate molar



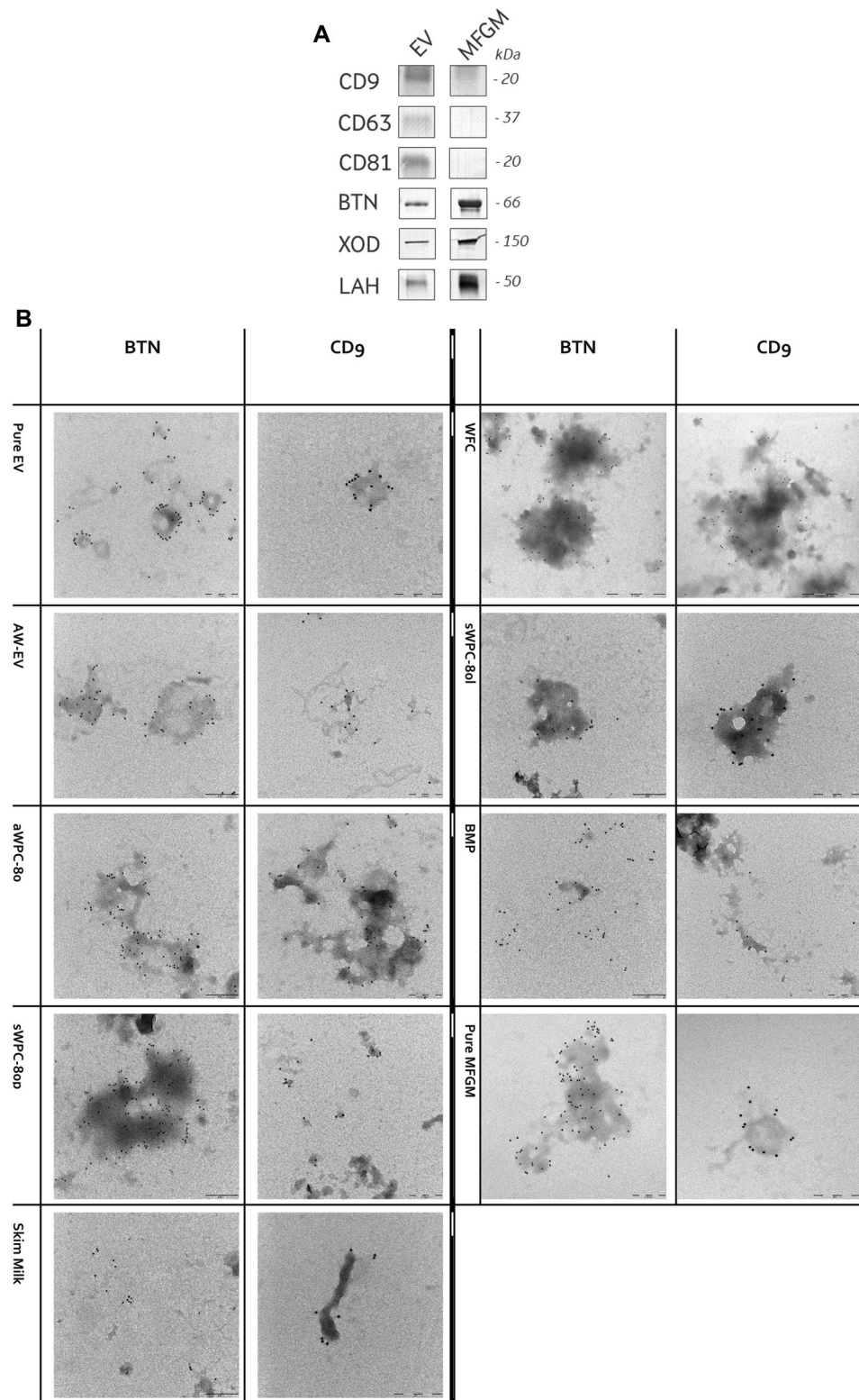


**FIGURE 4** | Membrane markers for EV and MFGM. (A) EVs and MFGM were assessed for the presence of six selected, well-established membrane markers by western blotting. It is observed that CD9, CD63 and CD81 are more strongly detected in the EV sample, with the opposite being observed for BTN, XOD and LAH. (B) Representative immunostain electron microscopy pictures of BTN and CD9 binding to a wide range of samples. All scalebars are 200 nm except for the WFC samples, where it is 500 nm. The black spots are the gold particles bound to the secondary antibodies, while the ‘shadows’ are sample material. An overview of the samples and accompanying labels can be found in Figure S2.

ratio of 4 in samples derived from sweet whey, highly similar to what has previously been described for MFGM (Mondy and Keenan 1993). This ratio was not conserved through the sample set with values varying from ~2 to ~10, indicating that at least one of the two proteins can be removed from the MFGM. A similar erratic pattern was observed for BTN/LAH and XOD/LAH molar ratios. We ascribe this to the fact that lactadherin (Yang et al. 2018) and xanthine oxidase/dehydrogenase are not integral membrane proteins and can dissociate from the phospholipid membrane, whereas BTN is an integral membrane protein that consistently follows the phospholipid membranes. Based on this data, we concluded that BTN was the best MFGM marker for this study.

We proceeded to test BTN and CD9 as markers for MFGM and EV material using immunostain electron microscopy (iEM) on the identical sample set as used for the quantitative MS analysis. A representative set of micrographs is seen in Figure 4B. These iEM data initially demonstrate a very good signal and a high degree of specificity of the used antibodies, as no unspecific/background staining is observed in any of the samples. Furthermore, we observe that the gold particles are in many places seemingly binding to the surface of the material, indicating that the antibodies are binding specifically to membrane proteins. This does not, however, necessarily imply that the MFGM and EVs are in their native state, only that MFGM and EV material is located in the apparent interfaces between the sample material and the surroundings, with an orientation that allows antibody binding to the membrane proteins. The low background and selective surface staining indicate that BTN and CD9 are present in all of the samples and do not dissociate from the membrane material.

### 3.4 | Quantification of EV and MFGM Material

In order to provide a robust relative quantification of the MFGM and EV material content in any sample, we used the molar ratio between BTN and CD9 as a measure of the EV and MFGM ratio. This single value has the advantage that no further experimental analyses are needed (e.g., phospholipid content, total solids content, protein content), and that samples are directly comparable, independent of the physical state (liquid or dry).

To test this idea, we compared the relative signals from BTN and CD9 using Western blotting, iEM and MS on the same sample set as mentioned above (see Figure S2 for processing overview and description). While the mode of signal generation and detection is very different between the three techniques, we hypothesized that the BTN/CD9 ratio should follow the same overall trend in all methods if the BTN/CD9 molar ratio represents a robust measure of relative MFGM and EV-derived material content. The BTN/CD9 molar ratio in the full sample set is plotted in Figure 5A. The same trend is identified from all the techniques, with pure MFGM and butter milk powder (BMP) having a very high BTN/CD9 molar ratio compared to all the other samples.

Due to the comparatively low experimental uncertainty in the MS data, we proceeded to work with this data. We extrapolated the individual BTN and CD9 values in a protein normalized format (Figure 5B, insert) between the pure EV and pure MFGM samples. While these two extrapolations can be used individually as standard curves to calculate the content of EV and MFGM

material in a given sample, utilizing the ratio between them removes the need for additional measurements (such as total solids, phospholipids, total protein, etc.), as they divide out when calculating the ratio). The resulting BTN/CD9 standard curve for the MS data is then seen in Figure 5B. The non-linearity of the curve is a result of the difference in the slope of the individual BTN and CD9 extrapolated data.

Comparing the measured BTN/CD9 ratios of the individual samples with the generated standard curve enables us to convert the BTN/CD9 ratio into a measure of how much of the phospholipid source in any given bovine-milk-derived sample (values are visualized in Figure 5C and listed in Table S3). As it assumes that the total phospholipid source is a binary sum of EV and MFGM material, the MFGM content can be calculated by subtracting the EV contribution from the total (100%).

In conclusion, based on the molar ratio of BTN and CD9 from MS data, it was evident that the industrial-scale isolated AW-EV fraction contained phospholipid membrane material deriving approximately 90% from milk EVs and 10% from MFGM. As such, the choice of input material (industrial acid whey depleted for casein) followed by a large-scale isolation procedure using sequential filtration resulted in an EV-enriched ingredient suitable for enrichment into IF.

## 4 | Discussion

We set out to produce a fraction enriched in bovine milk EV material through a patent-applied (EP20210361) serial filtration scheme using progressively smaller pores. This resulted in three main fractions that we have subjected to rigorous characterization, revealing that we have successfully isolated an enriched EV-material fraction with ~90% EV material present in the phospholipid source. Retrospectively, it is clear that acid whey (compared to sweet whey) is a very good starting material for this endeavour as the data in Figure 5C demonstrates that there is 20% more EV material present in the acid whey phospholipid pool compared to sweet whey. Furthermore, the expected size difference between MFGM and EV material has successfully been utilized to develop a filtration process to enrich a fraction for EV material. Our subsequent analysis provides a measure of the content of EV material, providing a very good addition to the analytical package presented by Mukhopadhyaya et al. (2021). The measured content of EV material in this work generally follows an expected trend. BMP is a sidestream from butter production. Since butter production is essentially a process of removing the MFGM from the MFG, butter milk should intuitively be enriched in MFGM material—as also demonstrated by the present data. Proceeding through the data, it is striking that sWPC-80, skim milk and WFC contain similar ratios of EV/MFGM material (highly similar BTN/CD9 ratio). The identical values for sWPC-80 and WFC indicate that while whey fat is concentrated, the production process of WFC has an identical influence on the two types of phospholipid assemblies, meaning that no separation of MFGM and EV material takes place through the production. Finally, aWPC-80 and the derived enriched EV fraction are very high in EV material content. Again, this is in line with the general expectations, as the casein precipitation by acid causes a significant amount of MFGs to co-precipitate and thereby

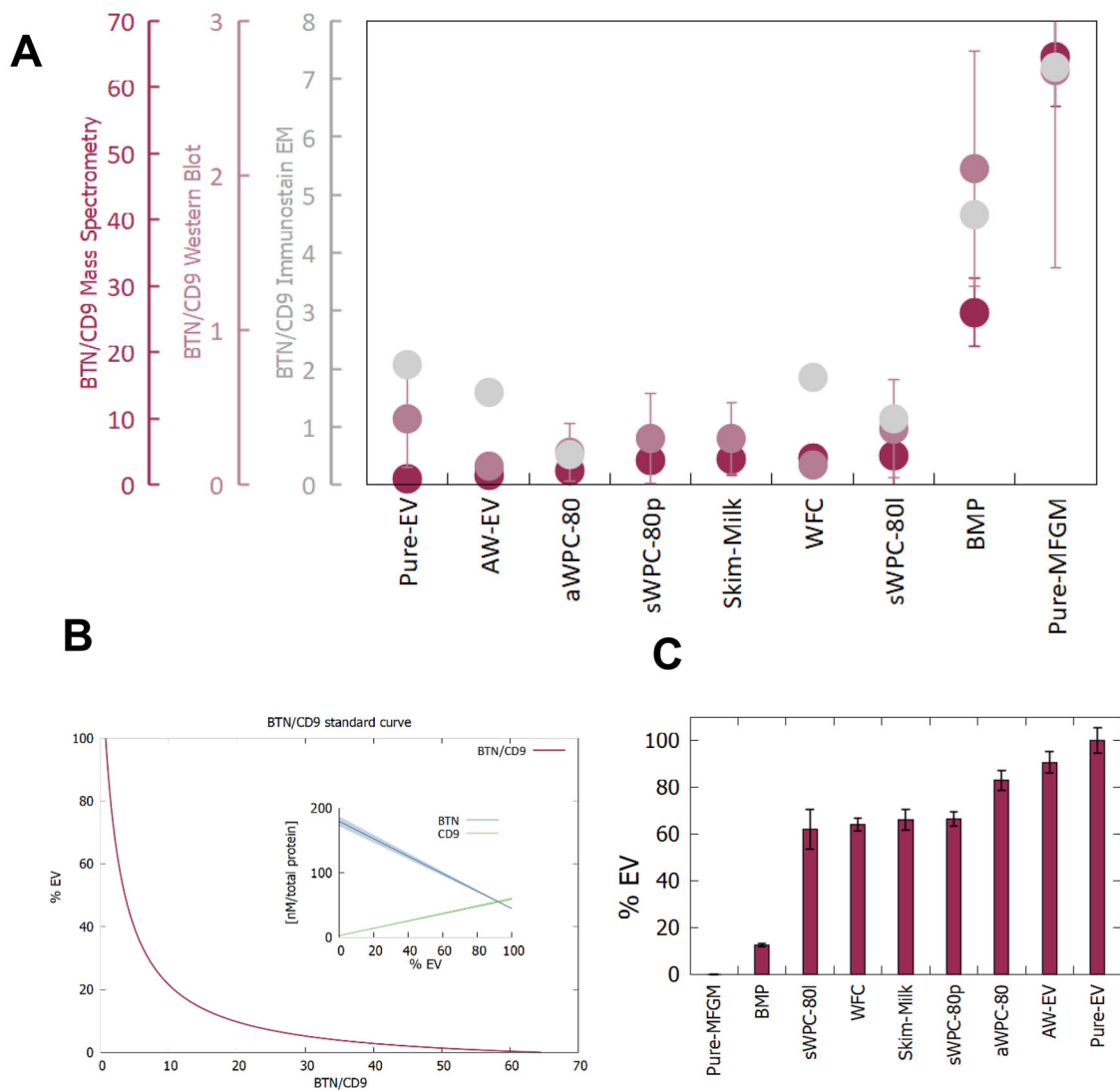


**FIGURE 5** | (A) BTN/CD9 ratio from MS, iEM and WB. (B) Calculated standard curve for the MS-based BTN/CD9 ratio (and individual extrapolated BTN and CD9 values are found in the insert). (C) Calculated values of EV presence by the MS-based standard curve. An overview and detailed explanation of the samples can be found in Figure S2. BTN, butyrophilin; iEM, immunogold electron microscopy.

changes the ratio of MFGM/EV material. Utilizing the average size difference between MFGM and EVs, it is from our present data evident that it is possible to produce an enriched fraction of EV material.

In our effort to analyse the content of EV material in our samples, we applied three analytical methods to quantify the selected membrane protein markers: peptides quantified by MS and two antibody-based methods (Western blotting and immunostain electron microscopy). Interestingly, all three methods suggested the same trend in the ratio of BTN/CD9 in different bovine milk-derived fractions/samples (Figure 5A), showing the highest ratio in purified MFGM. Initial attempts to identify applicable tetraspanin peptides for MS revealed difficulties, likely due to high protein hydrophobicity. It was, however, possible to generate useful MS data from CD9. Future assay optimizations may expand our knowledge on the content of CD63 and CD81 in these dairy fractions. In the same line of thought, other biological markers could likely be investigated for differentiating MFGM and EV material in an equivalent approach to the BTN/CD9 ratio. As

an example, bulk or individual miRNA might serve as a useable marker for EV material as long as they are not disrupted (Izumi et al. 2012). Using a ratio of one biological EV/MFGM marker compared to total phospholipid could also be speculated to provide an informative measure.

As expected, our Western blot analyses showed that it was possible to identify both CD9, CD63, and CD81 in the pure EV fraction (Figure 4A). However, recent studies suggest that these three EV markers are not equally good markers in dairy fractions subjected to processing. By Western blot analysis, the signals from especially CD63, and to a minor degree CD9, were shown to decrease in milk samples subjected to pasteurization and homogenization (Hansen et al. 2022; Kleinjan et al. 2021). These data could suggest that heating and mechanical processing of milk results in poorer antibody epitope recognition, thereby deteriorating the obtained signal—a finding that can be probed further by MS as denatured epitopes will not cause a signal lowering in this technique. An alternative explanation is that milk contains a heterogeneous population of EVs with subsets, enriched in



different tetraspanins, showing differences in, for example, heat sensitivity and thereby potential losses of subpopulations during milk processing. In general, investigating the effect of (industrial) processing on the vesicles and their subsequent morphology and retained molecular cargo is beyond this study but would be of value to further develop this class of novel ingredients.

Looking for BTN/CD9 ratios in the literature is complicated by the fact that most published data containing both BTN and CD9 quantitative measurements are from various types of label free MS analysis—giving a different response than the present method. One such label free study (Brink et al. 2020) provides easy access to their data and has a wide range of samples analysed. In here, the BTN/CD9 ratio from BMP (sample SM2) is 32.14, Butter serum concentrate (PL-20) is 37.05, MFGM-10 is 4.98, and a premium infant formula is 4.77. These numbers correspond very well with both the overall trend and values found in the present study (presented in Figure 5C). A further study by Lu et al. (2016) on large and small bovine MFGs finds BTN/CD9 ratios between 18.7 and 64.9 in samples from 7 cows. These values are in good agreement with the data from the present paper and suggest that their samples are indeed highly enriched MFGM samples. Interestingly, this data suggests a significant cow-to-cow variation. This individual variation could also originate from either the CD9 and/or BTN protein presence in the MFGM and EV material but could also be a consequence of individual EV size variation—causing more EV material to be co-purified with the MFGM material. Looking at EVs, Benmoussa et al. (2019) studied the isolation of bovine EVs by ultracentrifugation and demonstrated that the BTN/CD9 ratio decreases with increasing EV purity (BTN/CD9 = 2.05 for the 100KM sample versus BTN/CD9 = 9.04 for the 35KM sample), which is well in line with the findings in this paper. This trend is again also observed by Reinhardt et al. (2013), where the BTN/CD9 ratio is much higher for MFGM (110) than it is for EVs (14.6). A very interesting estimation of the EV production immediately post-partum comes from Samuel et al. (2017), demonstrating a decreasing BTN/CD9 ratio of a factor of two from 24 to 72 h post-partum (from 27.2 to 14.4), indicating a relative increase in EV secretion compared to MFGM (normalized spectral counts ‘NspC’ increase for both proteins during the 48 h indicating a general enrichment of MFGM and EV during the initial days post-partum). A further bovine study (Zhang et al. 2022) over the first 3 months of the lactation period suggests that the BTN/CD9 ratio is approximately constant, indicating that the majority of change in the MFGM/EV ratio takes place within the first days post-partum, well in line with the findings by Samuel et al. (2017).

Extending our understanding of the BTN/CD9 ratio to the available human literature is again complicated by the difference in the label-free methodologies employed. A study like Sari et al. (2021) investigated major pools ( $n \sim 30$ ) of milk from mothers in 8 different Chinese cities. Here the average BTN/CD9 ratio for the individual cities ranges between 4.3 and 13.4, indicating significant variation in the MFGM/EV ratio of the collected milk and potentially hinting towards geographical differences in the MFGM/EV ratio found in (human) milk. This finding is further corroborated by Zhu et al. (2021), where two individual donors have been monitored for 16 weeks. The BTN/CD9 ratio (calculated from values from their web interface at <https://milkprofiling.hecklab.com/>) is consistently  $\sim 6\times$

different between the donors (with donor 1 being the highest). Furthermore, this dataset seems to demonstrate that the BTN/CD9 ratio is constant for the duration of the 16-week study, consistent with what was observed for cows by Zhang et al. (2022).

Finally, dairy-phospholipid fractions like the ones studied in the present study have mainly been investigated regarding their influence on emulsification and digestive properties. Bach Korsholm Knudsen et al. (2021) have demonstrated the superior emulsification properties of the WFC and AW-EV samples used in this study—leading to improved fat digestion and triglyceride absorption in newborn formula-fed pigs, in comparison to soy lecithin. This could indicate that the beneficial properties of this type of phospholipid ingredient are a compounded effect of both biophysical and biochemical properties. Furthermore, the bioactivity of the Pure EV, WPC-80 and WPC samples used in this study has previously been evaluated (Ascanius et al. 2021) and found to reduce the inflammatory response in RAW264.7 cells. These findings support the role of EVs (and EV material) in likely aiding the protection of infants through effects on the intestinal immune system. This provides a positive foundation for future studies of the AW-EV fraction in order to fully evaluate the bioactivity.

## 5 | Conclusions

The present study represents a novel report of an enriched EV-material ingredient produced from acid whey on a significant scale. This ingredient has been described in high detail in relation to the source of phospholipids to confirm the enrichment of EVs with  $\sim 90\%$  of the phospholipids originating from EV material. Furthermore, we have introduced the BTN/CD9 molar ratio as a measure for the ratio between MFGM and EV material in any given milk-derived sample. This analytical approach has the potential to be used as a general measure of MFGM and EV material in any milk-derived sample (taking species-specific sequence variation into account).

In conclusion, the route of production and characterization of the ingredient enriched in EV material presented here enables the next step in the effort to eliminate differences between the composition of human breast milk and infant formulas—thereby hopefully aiding in minimizing the established difference between breast fed and formula fed infants. Further study into the preservation of the bioactive properties of milk-derived EVs is needed for novel ingredients like this to meet the global societal challenge of providing all individuals with the best possible life. Complementary to the development of ingredients like the one described here, significant efforts in documenting safety and efficacy will be required before commercial use of these types of ingredients can commence.

---

## Author Contributions

**Søren Roi Midtgaard:** data curation (lead), investigation (equal), project administration (supporting), writing—original draft (lead), writing—review and editing (lead). **Maria Stenum Hansen:** formal analysis (supporting), investigation (supporting), methodology (supporting), writing—review and editing (supporting). **Nikolaj Drachmann:** formal analysis



(lead), methodology (lead). **Xiaolu Geng**: formal analysis (supporting), methodology (equal). **Kristine Ingrid Marie Blans**: project administration (equal), writing—review and editing (supporting). **Manja Mahmens Fabricius Møbjerg**: formal analysis (equal). **Anny F. Frølund**: formal analysis (equal). **Jan Trige Rasmussen**: methodology (equal), writing—review and editing (supporting). **Marie Stampe Ostenfeld**: conceptualization (lead), funding acquisition (lead), project administration (equal), resources (equal), supervision (equal), writing—review and editing (equal).

## Acknowledgements

We acknowledge the Core Facility for Integrated Microscopy, Faculty of Health and Medical Sciences, University of Copenhagen, Denmark for their expertise in Electron Microscopy.

## Conflicts of Interest

All authors, except Jan Trige Rasmussen, have been or are employees of Arla Foods Ingredients—a company that produces whey-derived ingredients.

## Data Availability Statement

The data that support the findings of this study are available from the corresponding author upon reasonable request.

## References

Admyre, C., S. M. Johansson, K. R. Qazi, et al. 2007. “Exosomes With Immune Modulatory Features Are Present in Human Breast Milk.” *Journal of Immunology* 179, no. 3: 1969–1978.

Affolter, M., L. Grass, F. Vanrobaeys, B. Casado, and M. Kussmann. 2010. “Qualitative and Quantitative Profiling of the Bovine Milk Fat Globule Membrane Proteome.” *Journal of Proteomics* 73, no. 6: 1079–1088.

Anand, S., M. Samuel, S. Kumar, and S. Mathivanan. 2019. “Ticket to a Bubble Ride: Cargo Sorting Into Exosomes and Extracellular Vesicles.” *Biochimica et Biophysica Acta—Proteins and Proteomics* 1867, no. 12: 140203.

Anderson, J. W., B. M. Johnstone, and D. T. Remley. 1999. “Breast-Feeding and Cognitive Development: A Meta-Analysis.” *American Journal of Clinical Nutrition* 70, no. 4: 525–535.

Ascanius, S. R., M. S. Hansen, M. S. Ostenfeld, and J. T. Rasmussen. 2021. “Milk-Derived Extracellular Vesicles Suppress Inflammatory Cytokine Expression and Nuclear Factor- $\kappa$ B Activation in Lipopolysaccharide-Stimulated Macrophages.” *Dairy* 2, no. 2: 165–178.

Bach Korsholm Knudsen, K., C. Heerup, T. Røngaard Stange Jensen, et al. 2021. “Bovine Milk-Derived Emulsifiers Increase Triglyceride Absorption in Newborn Formula-Fed Pigs.” *Nutrients* 13, no. 2: 410.

Ballard, O., and A. L. Morrow. 2013. “Human Milk Composition: Nutrients and Bioactive Factors.” *Pediatric Clinics of North America* 60, no. 1: 49–74.

Bär, C., D. Mathis, P. Neuhaus, et al. 2019. “Protein Profile of Dairy Products: Simultaneous Quantification of Twenty Bovine Milk Proteins.” *International Dairy Journal* 97: 167–175.

Benmoussa, A., C. Gotti, S. Bourassa, C. Gilbert, and P. Provost. 2019. “Identification of Protein Markers for Extracellular Vesicle (EV) Subsets in Cow’s Milk.” *Journal of Proteomics* 192: 78–88.

Bhinder, G., J. M. Allaire, C. Garcia, et al. 2017. “Milk Fat Globule Membrane Supplementation in Formula Modulates the Neonatal Gut Microbiome and Normalizes Intestinal Development.” *Scientific Reports* 7: 45274.

Blans, K., M. S. Hansen, L. V. Sørensen, et al. 2017. “Pellet-Free Isolation of Human and Bovine Milk Extracellular Vesicles by Size-Exclusion Chromatography.” *Journal of Extracellular Vesicles* 6, no. 1: 1294340.

Brink, L. R., A. W. Herren, S. McMillen, et al. 2020. “Omics Analysis Reveals Variations Among Commercial Sources of Bovine Milk Fat Globule Membrane.” *Journal of Dairy Science* 103, no. 4: 3002–3016.

Buratta, S., L. Urbanelli, A. Tognoloni, et al. 2023. “Protein and Lipid Content of Milk Extracellular Vesicles: A Comparative Overview.” *Life* 13, no. 2: 1–14.

Bylund, G. n.d. *Dairy Processing Handbook*. Tetra Pak. ISBN 9789176111321.

Cavaletto, M., M. G. Giuffrida, and A. Conti. 2008. “Milk Fat Globule Membrane Components—A Proteomic Approach.” *Advances in Experimental Medicine and Biology* 606: 129–141. [https://doi.org/10.1007/978-0-387-74087-4\\_4](https://doi.org/10.1007/978-0-387-74087-4_4).

Chen, T., M. Y. Xie, J. J. Sun, et al. 2016. “Porcine Milk-Derived Exosomes Promote Proliferation of Intestinal Epithelial Cells.” *Scientific Reports* 6: 33862.

Chen, Y., Y. Zhao, Y. Yin, X. Jia, and L. Mao. 2021. “Mechanism of Cargo Sorting Into Small Extracellular Vesicles.” *Bioengineered* 12, no. 1: 8186–8201.

Claumarchirant, L., A. Cilla, E. Matencio, et al. 2016. “Addition of Milk Fat Globule Membrane as an Ingredient of Infant Formulas for Resembling the Polar Lipids of Human Milk.” *International Dairy Journal* 61: 228–238.

Demmelair, H., C. Prell, N. Timby, and B. Lönnerdal. 2017. “Benefits of Lactoferrin, Osteopontin and Milk Fat Globule Membranes for Infants.” *Nutrients* 9, no. 8: 1–22.

Fong, B. Y., and C. S. Norris. 2009. “Quantification of Milk Fat Globule Membrane Proteins Using Selected Reaction Monitoring Mass Spectrometry.” *Journal of Agricultural and Food Chemistry* 57, no. 14: 6021–6028.

Forbes, J. D., M. B. Azad, L. Vehling, et al. 2018. “Association of Exposure to Formula in the Hospital and Subsequent Infant Feeding Practices With Gut Microbiota and Risk of Overweight in the First Year of Life.” *JAMA Pediatrics* 172, no. 7: e181161.

Gu, Y., M. Li, T. Wang, et al. 2012. “Lactation-Related MicroRNA Expression Profiles of Porcine Breast Milk Exosomes.” *PLoS ONE* 7, no. 8: e43691.

Hansen, M. S., S. B. Gregersen, and J. T. Rasmussen. 2022. “Bovine Milk Processing Impacts Characteristics of Extracellular Vesicle Isolates Obtained by Size-Exclusion Chromatography.” *International Dairy Journal* 127: 105212.

Harzer, G., M. Haug, I. Dieterich, and P. R. Gentner. 1983. “Changing Patterns of Human Milk Lipids in the Course of the Lactation and During the Day.” *American Journal of Clinical Nutrition* 37, no. 4: 612–621.

Hata, T., K. Murakami, H. Nakatani, Y. Yamamoto, T. Matsuda, and N. Aoki. 2010. “Isolation of Bovine Milk-Derived Microvesicles Carrying mRNAs and microRNAs.” *Biochemical and Biophysical Research Communications* 396, no. 2: 528–533.

Heinemann, M. L., and J. Vykoukal. 2017. “Sequential Filtration: A Gentle Method for the Isolation of Functional Extracellular Vesicles.” *Methods in Molecular Biology* 1660: 33–41.

Izumi, H., N. Kosaka, T. Shimizu, K. Sekine, T. Ochiya, and M. Takase. 2012. “Bovine Milk Contains microRNA and Messenger RNA That Are Stable Under Degradative Conditions.” *Journal of Dairy Science* 95, no. 9: 4831–4841.

Izumi, H., M. Tsuda, Y. Sato, et al. 2015. “Bovine Milk Exosomes Contain microRNA and mRNA and Are Taken Up by Human Macrophages.” *Journal of Dairy Science* 98, no. 5: 2920–2933.

Kalra, H., R. J. Simpson, H. Ji, et al. 2012. “Vesiclepedia: A Compendium for Extracellular Vesicles With Continuous Community Annotation.” *PLoS Biology* 10, no. 12: 8–12.

Kleinjan, M., M. J. van Herwijnen, S. F. Libregts, R. J. van Neerven, A. L. Feitsma, and M. H. Wauben. 2021. “Regular Industrial Processing of Bovine Milk Impacts the Integrity and Molecular Composition of Extracellular Vesicles.” *Journal of Nutrition* 151, no. 6: 1416–1425.

- Lane, R. E., D. Korbie, M. Trau, and M. M. Hill. 2017. "Purification Protocols for Extracellular Vesicles." In *Extracellular Vesicles. Methods in Molecular Biology*, edited by W. Kuo and S. Jia, 111–130. Humana Press. [https://doi.org/10.1007/978-1-4939-7253-1\\_10](https://doi.org/10.1007/978-1-4939-7253-1_10).
- Lee, H., N. Zavaleta, S.-Y. Chen, B. Lönnerdal, and C. Slupsky. 2018. "Effect of Bovine Milk Fat Globule Membranes as a Complementary Food on the Serum Metabolome and Immune Markers of 6-11-Month-Old Peruvian Infants." *NPJ Science of Food* 2, no. 1: 6.
- Li, B., A. Hock, R. Y. Wu, et al. 2019. "Bovine Milk-Derived Exosomes Enhance Goblet Cell Activity and Prevent the Development of Experimental Necrotizing Enterocolitis." *PLoS ONE* 14, no. 1: e0211431.
- Li, F., S. S. Wu, C. L. Berseth, et al. 2019. "Improved Neurodevelopmental Outcomes Associated With Bovine Milk Fat Globule Membrane and Lactoferrin in Infant Formula: A Randomized, Controlled Trial." *Journal of Pediatrics* 215: 24–31.e8.
- Lönnerdal, B. 2010. "Bioactive Proteins in Human Milk: Mechanisms of Action." *Supplement, Journal of Pediatrics* 156, no. S2: S26–S30.
- Lu, J., N. Argov-Argaman, J. Anggrek, et al. 2016. "The Protein and Lipid Composition of the Membrane of Milk Fat Globules Depends on Their Size." *Journal of Dairy Science* 99, no. 6: 4726–4738.
- Martin, C. R., P.-R. Ling, and G. L. Blackburn. 2016. "Review of Infant Feeding: Key Features of Breast Milk and Infant Formula." *Nutrients* 8, no. 5: 279.
- Mecocci, S., F. Gevi, D. Pietrucci, et al. 2020. "Anti-Inflammatory Potential of Cow, Donkey and Goat Milk Extracellular Vesicles as Revealed by Metabolomic Profile." *Nutrients* 12, no. 10: 1–25.
- Mecocci, S., D. Pietrucci, M. Milanese, et al. 2021. "Transcriptomic Characterization of Cow, Donkey and Goat Milk Extracellular Vesicles Reveals Their Anti-Inflammatory and Immunomodulatory Potential." *International Journal of Molecular Sciences* 22, no. 23: 1–19.
- Mondy, B. L., and T. W. Keenan. 1993. "Butyrophilin and Xanthine Oxidase Occur in Constant Molar Proportions in Milk Lipid Globule Membrane But Vary in Amount With Breed and Stage of Lactation." *Protoplasma* 177: 32–36.
- Morozumi, M., H. Izumi, T. Shimizu, and Y. Takeda. 2021. "Comparison of Isolation Methods Using Commercially Available Kits for Obtaining Extracellular Vesicles From Cow Milk." *Journal of Dairy Science* 104, no. 6: 6463–6471.
- Mukhopadhyaya, A., J. Santoro, B. Moran, Z. Useckaite, and L. O'Driscoll. 2021. "Optimisation and Comparison of Orthogonal Methods for Separation and Characterisation of Extracellular Vesicles to Investigate How Representative Infant Milk Formula Is of Milk." *Food Chemistry* 353: 129309.
- Nieuwland, R., P. R. M. Siljander, J. M. Falcón-Pérez, and K. W. Witwer. 2022. "Reproducibility of Extracellular Vesicle Research." *European Journal of Cell Biology* 101, no. 5: 151226.
- Paolini, L., M. Monguió-Tortajada, M. Costa, et al. 2022. "Large-Scale Production of Extracellular Vesicles: Report on the "massivEVs" ISEV Workshop." *Journal of Extracellular Biology* 1, no. 10: e63.
- Patton, S., and T. W. Keenan. 1971. "The Relationship of Milk Phospholipids to Membranes of the Secretory Cell." *Lipids* 6: 58–61.
- Quigley, M. A., C. Carson, A. Sacker, and Y. Kelly. 2016. "Exclusive Breast-feeding Duration and Infant Infection." *European Journal of Clinical Nutrition* 70, no. 12: 1420–1427.
- Rahman, M. M., K. Shimizu, M. Yamauchi, et al. 2019. "Acidification Effects on Isolation of Extracellular Vesicles From Bovine Milk." *PLoS ONE* 14, no. 9: e0222613.
- Reinhardt, T. A., and J. D. Lippolis. 2006. "Bovine Milk Fat Globule Membrane Proteome." *Journal of Dairy Research* 73: 406–416.
- Reinhardt, T. A., J. D. Lippolis, B. J. Nonnecke, and R. E. Sacco. 2012. "Bovine Milk Exosome Proteome." *Journal of Proteomics* 75, no. 5: 1486–1492.
- Reinhardt, T. A., R. E. Sacco, B. J. Nonnecke, and J. D. Lippolis. 2013. "Bovine Milk Proteome: Quantitative Changes in Normal Milk Exosomes, Milk Fat Globule Membranes and Whey Proteomes Resulting From Staphylococcus Aureus Mastitis." *Journal of Proteomics* 82: 141–154.
- Samuel, M., D. Chisanga, M. Liem, et al. 2017. "Bovine Milk-Derived Exosomes From Colostrum Are Enriched With Proteins Implicated in Immune Response and Growth." *Scientific Reports* 7, no. 1: 1–10.
- Santoro, J., A. Mukhopadhyaya, C. Oliver, A. Brodtkorb, L. Giblin, and L. O'Driscoll. 2023. "An Investigation of Extracellular Vesicles in Bovine Colostrum, First Milk and Milk Over the Lactation Curve." *Food Chemistry* 401: 134029.
- Sanwlani, R., P. Fonseka, S. V. Chitti, and S. Mathivanan. 2020. "Milk-Derived Extracellular Vesicles in Inter-Organism, Cross-Species Communication and Drug Delivery." *Proteomes* 8, no. 2: 11. <https://doi.org/10.3390/proteomes8020011>.
- Sari, R. N., J. Pan, W. Zhang, et al. 2021. "Comparative Proteomics of Human Milk From Eight Cities in China During Six Months of Lactation in the Chinese Human Milk Project Study." *Frontiers in Nutrition* 8: 1–10.
- Schindelin, J., I. Arganda-Carreras, E. Frise, et al. 2012. "Fiji: An Open-Source Platform for Biological-Image Analysis." *Nature Methods* 9, no. 7: 676–682.
- Schneider, N., J. Hauser, M. Oliveira, et al. 2019. "Sphingomyelin in Brain and Cognitive Development: Preliminary Data." *eNeuro* 6, no. 4: 1–13.
- Sun, Q., X. Chen, J. Yu, K. Zen, C. Y. Zhang, and L. Li. 2013. "Immune Modulatory Function of Abundant Immune-Related microRNAs in Microvesicles From Bovine Colostrum." *Protein Cell* 4, no. 3: 197–210.
- Takumi, H., K. Kato, H. Nakanishi, et al. 2022. "Comprehensive Analysis of Lipid Composition in Human Foremilk and Hindmilk." *Journal of Oleo Science* 71, no. 7: 947–957.
- Théry, C., K. W. Witwer, E. Aikawa, et al. 2018. "Minimal Information for Studies of Extracellular Vesicles 2018 (MISEV2018): A Position Statement of the International Society for Extracellular Vesicles and Update of the MISEV2014 Guidelines." *Journal of Extracellular Vesicles* 7, no. 1: 1535750.
- Timby, N., M. Adamsson, E. Domellöf, et al. 2021. "Neurodevelopment and Growth Until 6.5 Years of Infants Who Consumed a Low-energy, Low-Protein Formula Supplemented With Bovine Milk Fat Globule Membranes: A Randomized Controlled Trial." *American Journal of Clinical Nutrition* 113, no. 3: 586–592.
- Timby, N., E. Domello, O. Hernell, and B. Lo. 2014. "Neurodevelopment, Nutrition, and Growth Until 12 mo of Age in Infants Fed a Low-Energy, Low-Protein Formula Supplemented With Bovine Milk Fat Globule Membranes : A Randomized Controlled Trial 1 –3." *American Journal of Clinical Nutrition* 99, no. 4: 860–868. <https://doi.org/10.3945/ajcn.113.064295.860>.
- Timby, N., O. Hernell, O. Vaarala, M. Melin, B. Lönnerdal, and M. Domellöf. 2015. "Infections in Infants Fed Formula Supplemented With Bovine Milk Fat Globule Membranes." *Journal of Pediatric Gastroenterology and Nutrition* 60, no. 3: 384–389.
- van Herwijnen, M. J. C., T. A. P. Driedonks, B. L. Snoek, et al. 2018. "Abundantly Present miRNAs in Milk-Derived Extracellular Vesicles Are Conserved Between Mammals." *Frontiers in Nutrition* 5: 81.
- Van Herwijnen, M. J. C., M. J. van Herwijnen, M. I. Zonneveld, and S. Goerdal. 2016. "Comprehensive Proteomic Analysis of Human Milk-derived Extracellular Vesicles Unveils a Novel Functional Proteome Distinct From Other Milk Components." *Molecular & Cellular Proteomics* 15, no. 11: 3412–3423.
- van Sadelhoff, J. H. J., D. Mastorakou, H. Weenen, B. Stahl, J. Garssen, and A. Hartog. 2018. "Short Communication: Differences in Levels of Free Amino Acids and Total Protein in Human Foremilk and Hindmilk." *Nutrients* 10, no. 12: 1828.
- Wadenpohl, T., M. Shein, J. Steinberg, J. B. Lehmann, A. K. Schütz, and S. Jung. 2024. "Economical Large-scale Purification of Extracellular Vesicles From Urine." *Separation and Purification Technology* 335: 126155.

- Welsh, J. A., D. C. I. Goberdhan, L. O'Driscoll, et al. 2023. "Minimal Information for Studies of Extracellular Vesicles (MISEV2023): From Basic to Advanced Approaches." *Journal of Extracellular Vesicles* 13, no. 2: e12404.
- Wooding, F. B. P. 1974. "Milk Fat Globule Membrane Material in Skim-Milk." *Journal of Dairy Research* 41: 331–337.
- World Health Assembly, 55. 2002. Infant and Young Child Nutrition: Global Strategy on Infant and Young Child Feeding: Report by the Secretariat. WHA55.
- Yang, Y., Y. Hong, E. Cho, G. B. Kim, and I. S. Kim. 2018. "Extracellular Vesicles as a Platform for Membrane-Associated Therapeutic Protein Delivery." *Journal of Extracellular Vesicles* 7, no. 1: 1440131.
- Yuan, R., Y. Zhou, G. F. Arias, and D. P. Dittmer. 2023. "Extracellular Vesicle Isolation by a Tangential-Flow Filtration-Based Large-Scale Purification Method." *Methods in Molecular Biology (Clifton, N.J.)* 2668: 45–55. [https://doi.org/10.1007/978-1-0716-3203-1\\_5](https://doi.org/10.1007/978-1-0716-3203-1_5).
- Zavaleta, N., A. S. Kvistgaard, G. Graverholt, et al. 2011. "Efficacy of an MFGM-Enriched Complementary Food in Diarrhea, Anemia, and Micronutrient Status in Infants." *Journal of Pediatric Gastroenterology and Nutrition* 53, no. 5: 561–568.
- Zhang, L., S. Boeren, J. Heck, J. Vervoort, P. Zhou, and K. Hettinga. 2022. "First Insight Into the Variation of the Milk Serum Proteome Within and Between Individual Cows." *Dairy* 3, no. 1: 47–58.
- Zhu, J., K. A. Dingess, M. Mank, B. Stahl, and A. J. R. Heck. 2021. "Personalized Profiling Reveals Donor- And Lactation-Specific Trends in the Human Milk Proteome and Peptidome." *Journal of Nutrition* 151, no. 4: 826–839.
- Zulewska, J., M. Newbold, and D. M. Barbano. 2009. "Efficiency of Serum Protein Removal From Skim Milk With Ceramic and Polymeric Membranes at 50°C." *Journal of Dairy Science* 92, no. 4: 1361–1377.

### Supporting Information

Additional supporting information can be found online in the Supporting Information section.